INTERNATIONAL JOURNAL FOR NUMERICAL METHODS IN FLUIDS
Int. J. Numer. Meth. Fluids 2005; **48**:819–833
Published online 24 March 2005 in Wiley InterScience (www.interscience.wiley.com). DOI: 10.1002/fld.957

Shape optimization of a body located in low Reynolds number flow

Hiroko Yagi and Mutsuto Kawahara*,†

Department of Civil Engineering, Chuo University, Kasuga 1-13-27, Bunkyo-ku, Tokyo 112-8551, Japan

SUMMARY

The purpose of this study is to perform a numerical application of the shape optimization formulation of a body located in an incompressible viscous flow field. The formulation is based on an optimal control theory in which a performance function of the fluid force is introduced. The performance function should be minimized satisfying the state equation. This problem can be transformed into the minimization problem without constraint condition by the Lagrange multiplier method and the adjoint equations using adjoint variables corresponding to the state equations. As a numerical study, the drag force minimization problem in the steady Stokes flow, which means approximated equation of the low Reynolds number Navier–Stokes equation is carried out. After that, the unsteady Navier–Stokes flow is analysed. As the minimization algorithm, the steepest descent method is successfully applied. Copyright © 2005 John Wiley & Sons, Ltd.

KEY WORDS: optimal control theory; finite element method; Lagrange multiplier; Navier–Stokes equation; mixed interpolation; steepest descent method; fluid forces

1. INTRODUCTION

The shape design of a body subjected to the minimum drag force has long been a challenging objective in the study of fluid dynamics. Computational fluid dynamics (CFD) has played an important role in the design process since its introduction to the study of fluid flow. CFD makes it possible to solve the shape optimization problem which is not based on experience and experiments. The shape optimization problem can be transformed into the minimization problem without constraint condition by the Lagrange multiplier method and the adjoint equations using adjoint variables to state variables of the state equations.

Pironneau [1–3] proposed the method of changing shape optimally using the gradient which is determined by taking variation with respect to coordinate. In an optimal control theory, control value which makes phenomenon an optimal state is solved. In this theory, performance

*Correspondence to: Mutsuto Kawahara, Department of Civil Engineering, Faculty of Science and Engineering, Chuo University, Kasuga 1-chome 13, Bunkyo-ku, Tokyo 112-8551, Japan.
†E-mail: kawa@civil.chuo-u.ac.jp

Received 7 March 2004
Revised 24 January 2005
Accepted 31 January 2005

function should be introduced. If the performance function is minimized, the state is optimized, and then a control value can be obtained. In case of the optimal control problem with constraint condition, the performance function should be minimized satisfying the state equation. Combination of CFD and the optimal control theory is expected to reduce computational time and cost. In this study, the fluid forces are directly included in the performance function. For the shape optimization, coordinate of the body can be taken as the control variable [4, 5]. Among optimization algorithm, the steepest descent methods are well-known optimization algorithms, which probe the optimum by calculating the local gradient information.

2. STATE EQUATION

Consider a typical problem described in Figure 1, in which a solid body B with the boundary Γ_B, is located in an external flow. Let Γ denote the boundary of Ω, suppose that an incompressible viscous flow occupies Ω. In this paper, indicial notation and summation convection with repeated indices are used to describe equation. The state equation of the flow can be written by the Navier–Stokes equation in the non-dimensional form,

$$\dot{u}_i + u_j u_{i,j} + p_{,i} - \nu(u_{i,j} + u_{j,i})_{,j} = 0 \quad \text{in } \Omega \tag{1}$$

$$u_{i,i} = 0 \quad \text{in } \Omega \tag{2}$$

where u_i, p and ν are the velocity, pressure, and the viscosity coefficient ($\nu = 1/Re$), respectively, in which Re is the Reynolds number.

Suppose that the boundary conditions are as follows:

$$u_i = \hat{u}_i \quad \text{on } \Gamma_U \tag{3}$$

$$t_1 = 0, \quad u_2 = 0 \quad \text{on } \Gamma_S \tag{4}$$

$$u_i = 0 \quad \text{on } \Gamma_B \tag{5}$$

$$t_i = 0 \quad \text{on } \Gamma_D \tag{6}$$

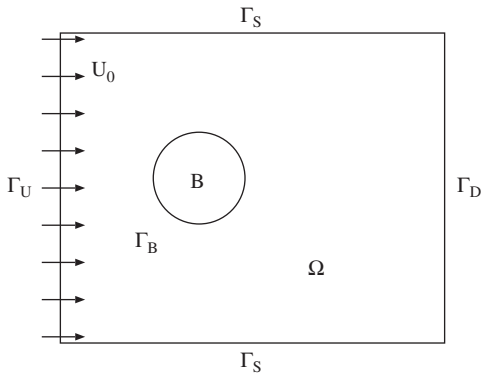

Figure 1. Analytical domain and boundary condition.

where

$$t_i = \{-p\delta_{ij} + \nu(u_{i,j} + u_{j,i})\}n_j \tag{7}$$

in which t_i is traction, and n_j is unit vector of outward normal to Γ, respectively. The fluid forces subjected to the body are denoted by F_i, where F_1 and F_2 are a drag and lift forces, respectively. The fluid force F_i is obtained by integrating the traction t_i on the boundary Γ_B,

$$F_i = -\int_{\Gamma_B} t_i \, \mathrm{d}\Gamma \tag{8}$$

3. APPROXIMATION

3.1. Mixed interpolation

The weighted residual equation of the basic equation is written as follows:

$$\int_\Omega w_i \dot{u}_i \, \mathrm{d}\Omega + \int_\Omega w_i u_j u_{i,j} \, \mathrm{d}\Omega + \int_\Omega w_{i,j}\{-p\delta_{ij} + \nu(u_{i,j} + u_{j,i})\} \, \mathrm{d}\Omega = \int_\Gamma w_i t_i \, \mathrm{d}\Gamma \tag{9}$$

$$\int_\Omega q u_{i,i} \, \mathrm{d}\Omega = 0 \tag{10}$$

where w_i and q are weighting functions.

As for the spatial discretization of the bubble function interpolation is used [6–8]. The mixed interpolation for the momentum and pressure equations can be expressed in the following form:

(1) The bubble function interpolation for velocity

$$\begin{aligned} u_i &= \mathbf{\Phi}_1 u_{i1} + \mathbf{\Phi}_2 u_{i2} + \mathbf{\Phi}_3 u_{i3} + \mathbf{\Phi}_4 \tilde{u}_{i4} \\ \tilde{u}_{i4} &= u_{i4} - \tfrac{1}{3}(u_{i1} + u_{i2} + u_{i3}) \\ \mathbf{\Phi}_1 &= \eta_1, \quad \mathbf{\Phi}_2 = \eta_2, \quad \mathbf{\Phi}_3 = \eta_3, \quad \mathbf{\Phi}_4 = 27\eta_1\eta_2\eta_3 \end{aligned} \tag{11}$$

and

(2) The linear interpolation for pressure

$$\begin{aligned} p &= \mathbf{\Psi}_1 p_1 + \mathbf{\Psi}_2 p_2 + \mathbf{\Psi}_3 p_3 \\ \mathbf{\Psi}_1 &= \eta_1, \quad \mathbf{\Psi}_2 = \eta_2, \quad \mathbf{\Psi}_3 = \eta_3 \end{aligned} \tag{12}$$

where $\mathbf{\Phi}_\alpha$ ($\alpha = 1, 4$) is the bubble function in four-node triangular element, $\mathbf{\Psi}_\lambda$ ($\lambda = 1, 3$) is the linear interpolation for pressure in three-node triangular element and $u_{i\alpha}$ and p_λ represent the nodal values at the αth node of each finite element as shown in Figure 2.

In the present analysis, the criteria of the stabilized parameter for the steady problem is used, in which the discretized form derived by the bubble function element is equivalent to

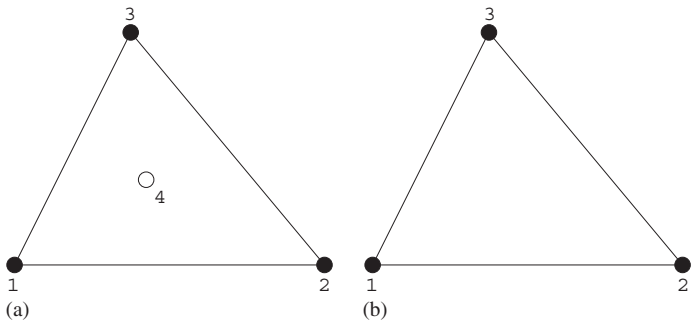

Figure 2. Mixed interpolation function: (a) Bubble function interpolation; and (b) linear interpolation.

those by the SUPG method [9]. In the bubble function element for the steady problem, the stabilized parameter τ_{eB} which determines the magnitude of the streamline stabilized term can be given by

$$\tau_{eB} = \frac{\langle \phi_e, 1 \rangle^2_{\Omega_e}}{\nu \| \phi_{e,j} \|^2_{\Omega_e} A_e} \tag{13}$$

where $\langle u', v' \rangle_{\Omega_e} = \int_{\Omega_e} u'v' \, \mathrm{d}\Omega$, $\|u'\|^2_{\Omega_e} = \int_{\Omega_e} u'u' \, \mathrm{d}\Omega$ and $A_e = \int_{\Omega_e} \mathrm{d}\Omega$. From the criteria of the stabilized parameter in the SUPG method, an optimal parameter τ_{eS} can be chosen as

$$\tau_{eS} = \left[\left(\frac{2|u'_i|}{h_e} \right)^2 + \left(\frac{4\nu}{h_e^2} \right)^2 \right]^{-1/2} \tag{14}$$

where h_e is an element size.

Generally, Equation (13) is not equal to Equation (14). The bubble function that gives optimal viscosity satisfies the following equation expressed by the stabilized operator control parameter ν:

$$\frac{\langle \phi_e, 1 \rangle^2_{\Omega_e}}{\nu \| \phi_{e,j} \|^2_{\Omega_e} A_e} = \tau_{eS} \tag{15}$$

It is shown that Equation (15) adds stabilized operator control term in Equation (16) only at the barycentre point to the equation of motion;

$$\sum_{e=1}^{N_e} \nu' \| \phi_{e,j} \|^2_{\Omega_e} b_e \tag{16}$$

where N_e and b_e are the total number of elements and barycentre point.

3.2. Finite element equation

The finite element equation yields as follows:

$$M\dot{U}_i + A^j(U_j)U_i - C^i P + D^{ij}U_i + D^{ji}U_j = T_i \quad \text{in } \Omega \tag{17}$$

$$C^{i^{\mathrm{T}}} U_i = 0 \quad \text{in } \Omega \tag{18}$$

where

$$M = \int_{\Omega} N_\alpha N_\beta \, \mathrm{d}\Omega$$

$$D^{ji} = \int_{\Omega} N_{\alpha,j} N_{\beta,i} \, \mathrm{d}\Omega$$

$$A^i(U_i) = \int_{\Omega} N_\alpha N_\beta U_i N_{\gamma,i} \, \mathrm{d}\Omega$$

$$C^i = \int_{\Omega} N_{\alpha,i} N_\beta \, \mathrm{d}\Omega$$

$$T_i = \int_{\Gamma_B} \eta t_i^h \, \mathrm{d}\Gamma$$

in which N and η are the interpolation function for each element of domain Ω and boundary Γ, respectively. The approximated velocity and pressure at each nodal points are denoted by U_i and P, respectively.

3.3. Temporal discretization

The Crank–Nicolson method is used for the temporal discretization of the state equation.

$$M\frac{U_i^{n+1} - U_i^n}{\Delta t} + A^j(U_j^{n+(1/2)})U_i^{n+(1/2)} - C^i P^{n+1} + D^{jj}U_i^{n+(1/2)} + D^{ji}U_j^{n+(1/2)} = T_i \quad \text{in } \Omega \tag{19}$$

$$C^{i^{\mathrm{T}}} U_i^{n+1} = 0 \quad \text{in } \Omega \tag{20}$$

where

$$U_i^{n+(1/2)} = \tfrac{1}{2}(U_i^n + U_i^{n+1}) \tag{21}$$

In this equation, advection term is nonlinear. It is necessary to spend long calculation time to solve nonlinear equation. Then, in this research $U_j^{n+(1/2)}$ in the advection term is approximated using average velocity of U_j^n in each finite element.

$$A^i(U_i) = \bar{U}_i^n \int_{\Omega} N_\alpha N_{\beta,i} \, \mathrm{d}\Omega$$

4. FORMULATION OF SHAPE OPTIMIZATION

In this paper, the shape optimization is defined as follows. Find the coordinate of the body, which expresses the shape to minimize the fluid force subjected to the body under the constraints of the Navier–Stokes equations.

4.1. Volume constraint

The shape of the body should be optimized keeping the volume constant. The volume should be kept in each iteration cycle. To keep the volume of the body is equal to keep the volume of the whole domain to be analysed. The volume constraint equation yields as follows:

$$\sum_{e=1}^{m}(a_e(x_i)) - A_0 = 0 \tag{22}$$

where $a_e(x_i)$ is the volume of each element and A_0 is the volume of the initial domain.

4.2. Performance function

In this paper, a fluid force control problem is performed. The performance function J is defined by the square sum of the computed fluid force, i.e.

$$J = \frac{1}{2}\int_{t_1}^{t_2}(q_1F_1^2 + q_2F_2^2)\,\mathrm{d}t \tag{23}$$

where q_1 and q_2 are the weighting parameter of the drag and lift forces, respectively. The performance function should be minimized satisfying Equations (17) and (18). The Lagrange multiplier method is suitable for the optimal control problem with the constraint conditions [10]. The Lagrange multipliers for Equations (17) and (18) and volume constraint are defined as adjoint velocity U_i^*, pressure P^* and Lagrange multiplier of the volume constraint equation λ. This problem can be transformed into the stationary problem of the extended performance function J^* which can be obtained by adding the dot product between adjoint velocity U_i^*, pressure P^* and λ and state Equations (17) and (18) to the original performance function as follows:

$$\begin{aligned} J^* = {} & \frac{1}{2}\int_{t_1}^{t_2}(q_1F_1^2 + q_2F_2^2)\,\mathrm{d}t \\ & - \int_{t_1}^{t_2} U_i^{*\mathrm{T}}(MU_i + A^j(U_j)U_i - C^iP + D^{jj}U_i + D^{ji}U_j - T_i)\,\mathrm{d}t \\ & + \int_{t_1}^{t_2} P^{*\mathrm{T}}C^{i^{\mathrm{T}}}U_i\,\mathrm{d}t + \lambda\left\{\sum_{e=1}^{m}(a_e(x_i)) - A_0\right\} \end{aligned} \tag{24}$$

where the approximated trial function of the velocity and pressure are denoted by U_i and P, respectively.

4.3. Stationary condition

The optimal control problem with the constraint condition of Equations (1) and (2) results in solving a stationary condition of the extended performance function J^* instead of the original performance function J. The stationary condition of the extended performance function J^* is that the first variation yields zero, which is expressed as follows:

$$\delta J^* = -\int_{t_1}^{t_2} \delta U_i^{*\mathrm{T}}(MU_i + A^j(U_j)U_i - C^iP + D^{jj}U_i + D^{ji}U_j - T_i)\,\mathrm{d}t$$

$$+\int_{t_1}^{t_2} \delta P^{*\mathrm{T}} C^{i^{\mathrm{T}}} U_i \,\mathrm{d}t - \int_{t_1}^{t_2} \delta U_i^{\mathrm{T}} (M U_i^* A^{j^{\mathrm{T}}}(U_j) U_i^* - C^i P^* + v(D^{jj^{\mathrm{T}}} U_i^* + D^{ij^{\mathrm{T}}} U_j^*)) \,\mathrm{d}t + \int_{t_1}^{t_2} \delta P^{\mathrm{T}} C^{i^{\mathrm{T}}} U_i^* \,\mathrm{d}t + \int_{t_1}^{t_2} \delta T_i^{\mathrm{T}} (U_i^* - q_i F_i) \,\mathrm{d}t + \delta\lambda^{\mathrm{T}} \left\{ \sum_{e=1}^{m} (a_e(x_i)) - A_0 \right\} + \delta X_i^{\mathrm{T}} G_i \tag{25}$$

where

$$G_k = -\int_{t_1}^{t_2} U_i^{*\mathrm{T}} \left(\frac{\partial M U_i}{\partial X_k} U_i + \frac{\partial A^j(U_j)}{\partial X_k} U_i - \frac{\partial C^i}{\partial X_k} P + \frac{\partial D^{jj}}{\partial X_k} U_i + \frac{\partial D^{ji}}{\partial X_k} U_j - \frac{\partial T_i}{\partial X_k} \right) \mathrm{d}t + \int_{t_1}^{t_2} P^{*\mathrm{T}} \frac{\partial C^{i^{\mathrm{T}}}}{\partial X_k} U_i \,\mathrm{d}t + \lambda^{\mathrm{T}} \frac{\partial}{\partial X_k} \sum_{e=1}^{m} a_e(X_i) \tag{26}$$

in which G_k and X_k gives the gradient of the extended performance function and coordinate of body boundary, respectively. Setting each term equal to zero to satisfy the optimal condition, following equations are obtained:

$$M\dot{U}_i + A^j(U_j)U_i - C^i P + D^{jj} U_i + D^{ji} U_j = T_i \quad \text{in } \Omega \tag{27}$$

$$C^{i^{\mathrm{T}}} U_i = 0 \quad \text{in } \Omega \tag{28}$$

$$M^{\mathrm{T}} \dot{U}_i^* + A^{j^{\mathrm{T}}}(U_j) U_i^* - C^i P^* + D^{jj^{\mathrm{T}}} U_i^* + D^{ji^{\mathrm{T}}} U_j^* = T_i \quad \text{in } \Omega \tag{29}$$

$$C^{i^{\mathrm{T}}} U_i^* = 0 \quad \text{in } \Omega \tag{30}$$

$$q_i F_i - U_i^* = 0 \quad \text{on } \Gamma_B \tag{31}$$

$$\sum_{e=1}^{m} (a_e(x_i)) - A_0 = 0 \quad \text{in } \Omega \tag{32}$$

$$G_i = 0 \quad \text{in } \Omega \tag{33}$$

where U_i, P, U_i^*, P^*, and λ should be solved satisfying Equations (26)–(32). The optimal condition of the present problem can be given as follows:

$$\frac{\partial J^*}{\partial X_i} = G_i = 0 \tag{34}$$

5. MINIMIZATION

5.1. Steepest descent method

The steepest descent method is applied to the minimization in this paper. In this method, a modified performance function, which can be obtained adding a penalty term to the perfor-

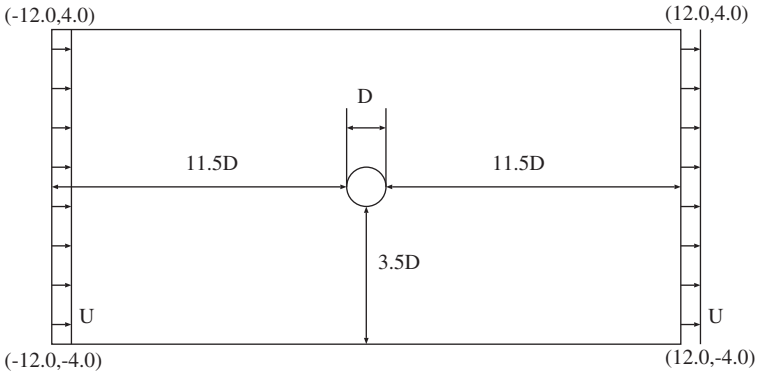

Figure 3. Analytical domain.

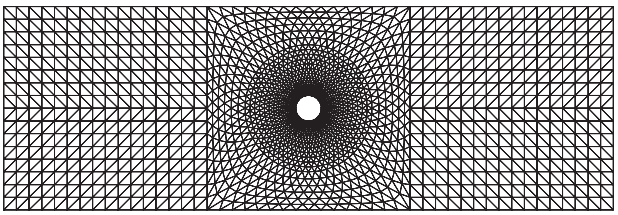

Figure 4. Finite element mesh.

mance function expressed by Equation (23) is introduced. The modified performance function J^{**} is

$$J^{**(k)} = J^{*(k)} + \frac{1}{2}\int_{\Gamma_B} W(X_i^{(k+1)} - X_i^{(k)})^2 \, \mathrm{d}\Gamma \tag{35}$$

where k is the iteration number for minimization, W is weighting parameter. If the modified performance function J^{**} converge to the minimum, the penalty term must be zero. To minimize the modified performance function J^{**} is equal to minimize the extended performance function J^{*}.

Let X_i be the optimal solution of the coordinate, then the following equality should hold:

$$\frac{\partial J^{**(k)}}{\partial X_i^{(k)}} = 0 \tag{36}$$

and the renewed surface coordinates of body is calculated at each iteration step by the following equation:

$$WX_i^{(k+1)} = WX_i^{(k)} - \frac{\partial J^{*(k)}}{\partial X_i^{(k)}} \tag{37}$$

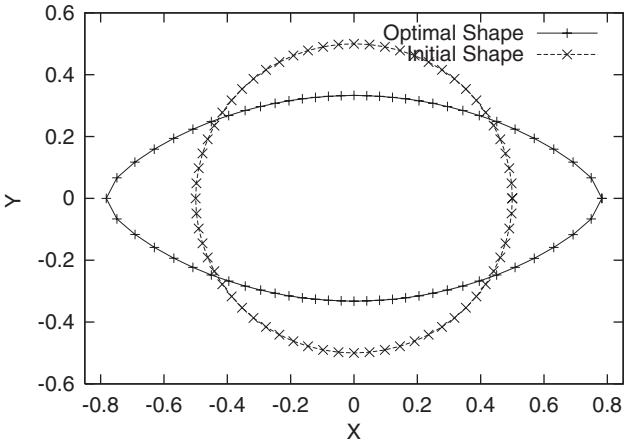

Figure 5. Initial shape body and optimal shape body.

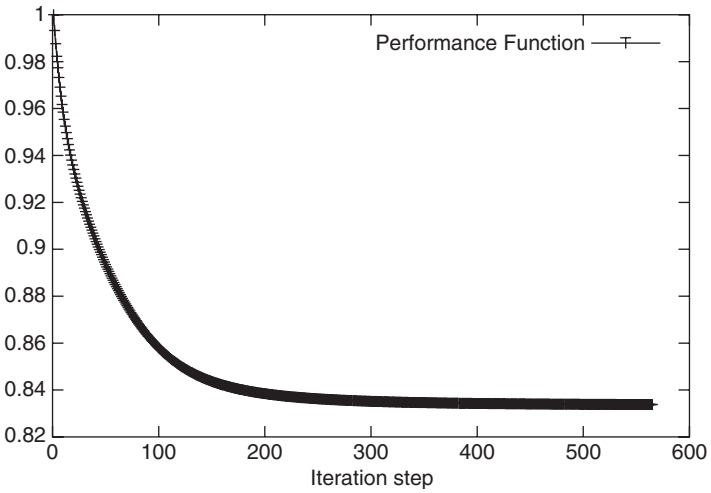

Figure 6. Performance function.

5.2. *Algorithm*

The following algorithm is employed for the computation.

1. Select initial surface coordinates $X_i^{(0)}$ in Ω.
2. Solve $u_i^{(0)}$, $p^{(0)}$ by Equations (26), (27) in Ω.
3. Compute $J^{(0)}$.
4. Solve $u_i^{*(0)}$, $p^{*(0)}$ by Equations (28)–(30) in Ω.
5. Compute $X_i^{(k)}$ by Equation (36).
6. Solve $u_i^{(k)}$, $p^{(k)}$ by Equations (26), (27) in Ω.
7. Compute $J^{(k)}$.

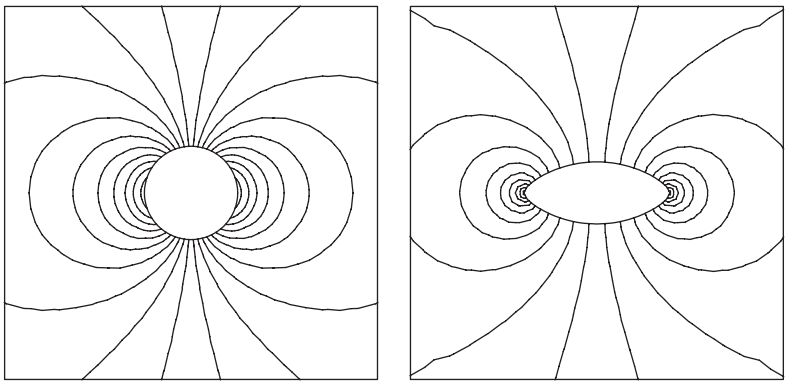

(a) (b)

Figure 7. Pressure distribution: (a) Initial shape; and (b) optimal shape.

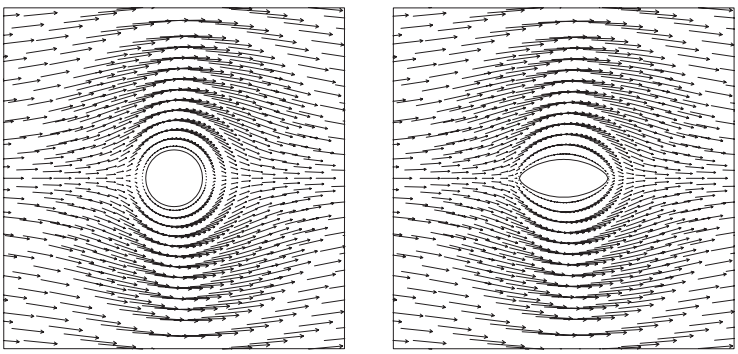

(a) (b)

Figure 8. Velocity vector distribution: (a) Initial shape; and (b) optimal shape.

8. If $|X_i^{(k)} - X_i^{(k-1)}| < \varepsilon$ then stop. Else solve $u_i^{*(k)}$, $p^{*(k)}$ by Equations (28)–(30) in Ω.
9. Go to 5.

6. NUMERICAL STUDIES

For numerical study, the drag minimization problem of a circular cylinder located in the viscous flow is analysed. The weighting parameter q_1 and q_2 are 1.0 and 0.0, respectively.

6.1. Case 1

For the state equation, the Stokes equation is applied.

$$p,i - v(u_{i,j} + u_{j,i})_{,j} = 0 \quad \text{in } \Omega$$
$$u_{i,i} = 0 \quad \text{in } \Omega$$

Figures 3 and 4 show the domain to be analysed and the finite element mesh.

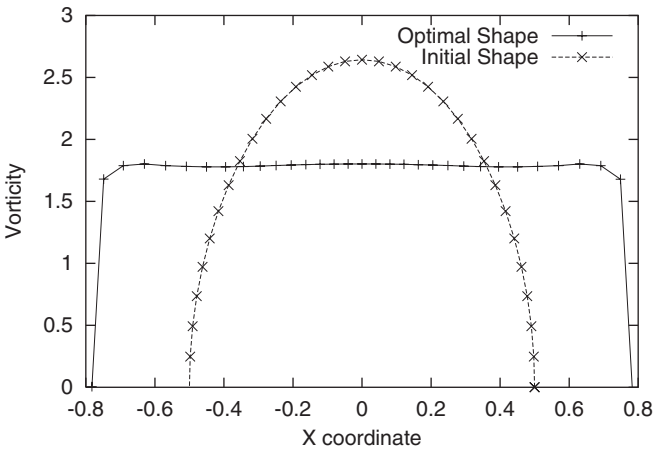

Figure 9. Vorticity distribution on surface of the body.

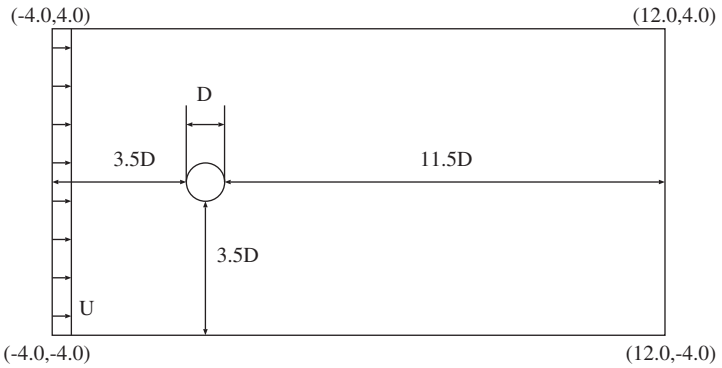

Figure 10. Analytical domain.

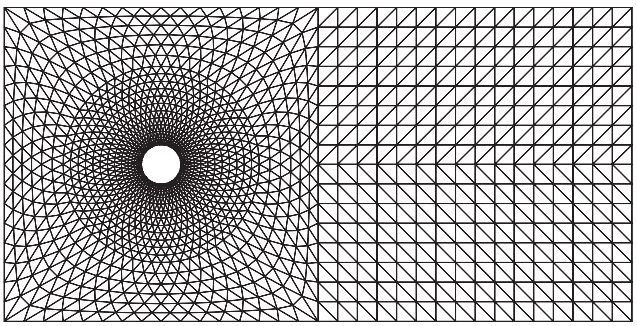

Figure 11. Finite element mesh.

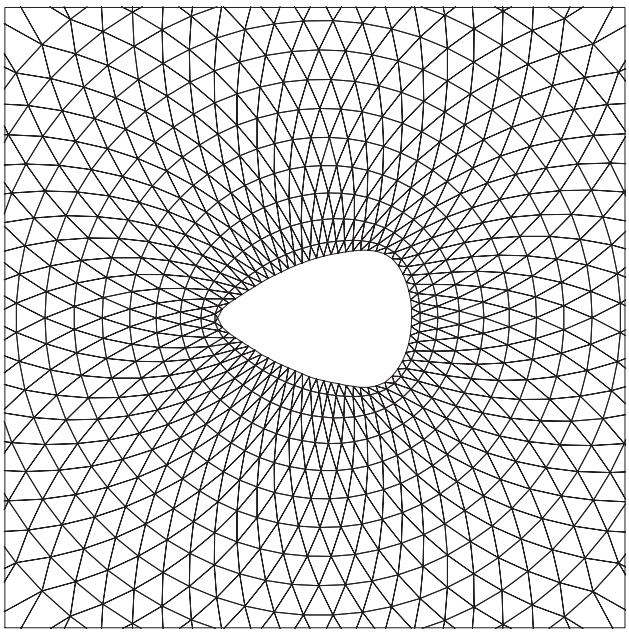

Figure 12. Finite element mesh of optimal shape ($Re = 100.0$).

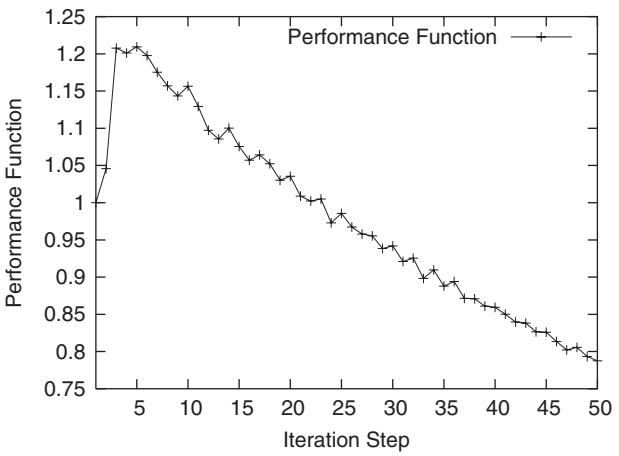

Figure 13. Performance function.

The Reynolds number is 0.1. Figure 5 represents the initial shape and a optimal shape of the body. Figure 6 shows history of the performance function. Figures 7 and 8 are pressure and velocity vector distributions. Figure 9 illustrates vorticity distribution on the surface of the body. It is clearly shown in Figure 9 that the Pironneau's necessary condition has been satisfied.

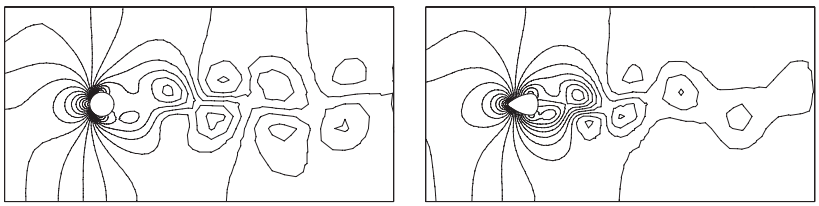

Figure 14. Pressure distribution: (a) Initial shape; and (b) optimal shape.

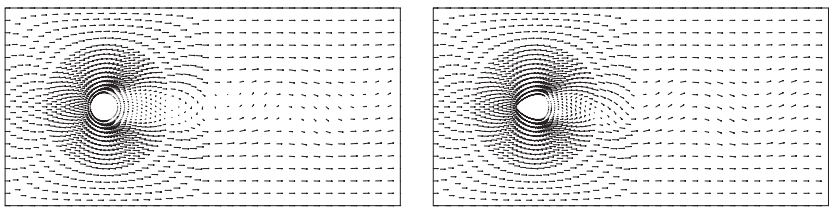

Figure 15. Velocity vector distribution: (a) Initial shape; and (b) optimal shape.

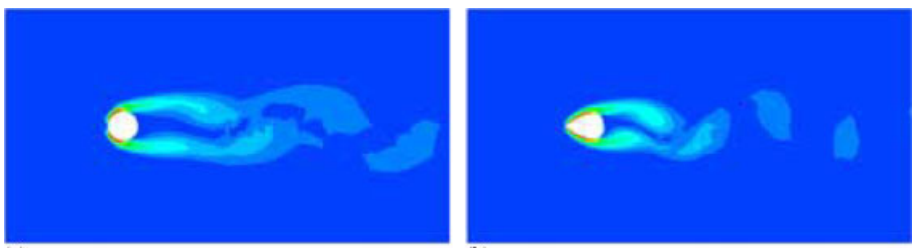

Figure 16. Vorticity distribution: (a) Initial shape; and (b) optimal shape.

6.2. *Case 2*

For the state equation, the Navier–Stokes equation is applied.

$$\dot{u}_i + u_j u_{i,j} + p,i - v(u_{i,j} + u_{j,i})_{,j} = 0 \quad \text{in } \Omega$$

$$u_{i,i} = 0 \quad \text{in } \Omega$$

Figures 10 and 11 show the domain to be analysed and the finite element mesh.

The Reynolds number is set at 100.0. Figure 12 represents the finite element mesh of the final optimal shape. Figure 13 shows history of the performance function. Figures 14 and 15 are pressure and velocity vector distributions. Figure 16 illustrates vorticity distribution. Generally, to minimize the wake, in which there is vorticity, the inswept shape which does not cause separation is defined as the optimal shape. However, in this case, the wake can be

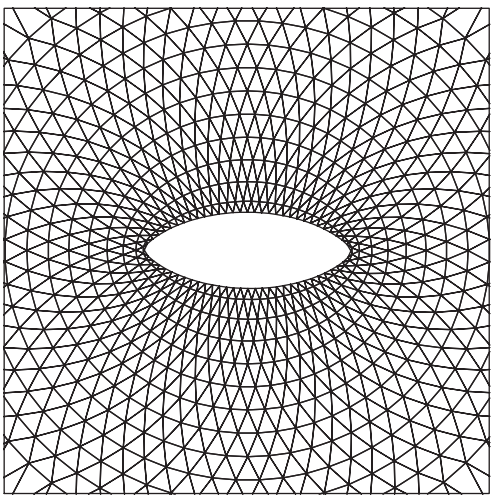

Figure 17. Finite element mesh of initial shape ($Re = 100.0$).

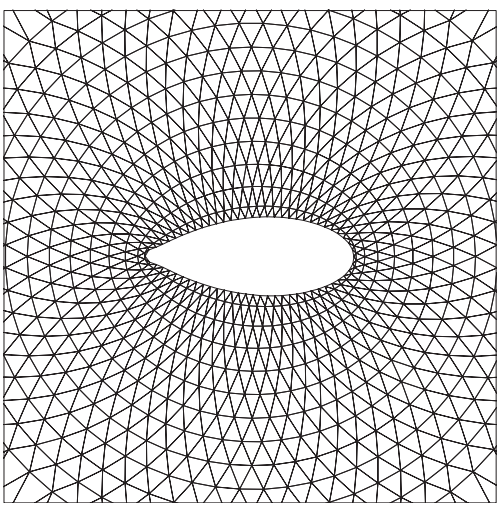

Figure 18. Finite element mesh of controlled shape ($Re = 100.0$).

minimized in the shape in Figure 12 which does not have inswept form. This seems because no separation has occurred around the circular cylinder.

6.3. Case 3

Optimal shape obtained at the Stokes flow is selected as the initial shape. Figures 17 and 18 show the finite element meshes of the initial and the controlled shapes which is intermediate shape in the computation. Figure 19 illustrates the gradient vectors. The shape is changing to the shape which is similar to the one obtained in Figure 12.

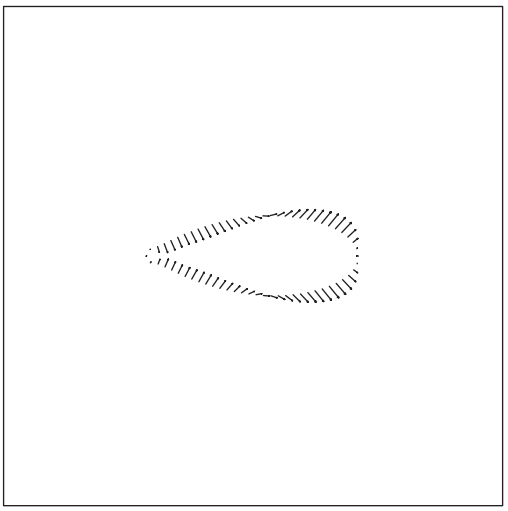

Figure 19. Gradient vectors ($Re = 100.0$).

7. CONCLUSION

In this paper, the shape optimization in the Stokes flow and the Navier–Stokes flow has been presented. The adjoint equation was derived from the gradient of the performance function. The steepest descent method is effectively used for the minimization algorithm. The operation of changing the body shape has started from the circle and the initial body shape obtained by the previous calculation. In the Stokes flow, the drag force is reduced about 17%. The Pironneau's necessary condition that the vorticity distribution on the surface of the body is almost constant is obtained. This method can be applied to the unsteady flow. In the optimal shape, wake has been controlled.

REFERENCES

1. Pironneau O. On optimum profiles in Stokes flow. *Journal of Fluid Mechanics* 1973; **59**(1):117–128.
2. Pironneau O. On optimum design in fluid mechanics. *Journal of Fluid Mechanics* 1974; **64**(1):97–110.
3. Pironneau O. *Optimal Shape Design for Elliptic Systems*. Springer: Berlin, 1983.
4. Ogawa Y, Kawahara M. Shape optimization a body located in incompressible viscous flow based on optimal control theory. *International Journal of Computational Fluid Dynamics* 2003; **17**(4):243–251.
5. Tashiro M, Kawahara M. Drag minimization problem using Lagrange multiplier method based on optimal control theory 2004, in press.
6. Brezzi F, Arnold DN, Fortin M. A stable finite element for the Stokes equations. *Calcolo* 1984; **21**(4):337–344.
7. Matsumoto J, Kawahara M. Stable shape identification for fluid-structure interaction problem using mini element. *Journal of Applied Mechanics* 2000; **3**:263–274.
8. Umetsu T, Matsumoto J, Kawahara M. Incompressible viscous flow analysis and adaptive finite element method using linear bubble function. *Journal of Applied Mechanics* 1999; **2**:223–232.
9. Franca LP, Huges TJR, Balestra M. A new finite element formulation for computational fluid dynamics: V. Circumventing the Babuska–Brezzi condition: a stable Petrov–Galerkin formulation of the Stokes problem accommodating equal order interpolation. *Computer Methods in Applied Mechanics and Engineering* 1986; **59**:85–99.
10. Maruoka A, Kawahara M. Optimal control in Navier–Stokes equation. *International Journal of Computational Fluid Dynamics* 1998; **9**:313–322.

